Extracellular lipids of *Candida albicans* biofilm induce lipid droplet formation and decreased response to a topoisomerase I inhibitor in dysplastic and neoplastic oral cells*

Freddy Humberto MARIN-DETT[1] (iD)
Jonatas Erick Maimoni CAMPANELLA[2] (iD)
Eliane TROVATTI[3] (iD)
Maria Célia BERTOLINI[2] (iD)
Carlos Eduardo VERGANI[4] (iD)
Paula Aboud BARBUGLI[1,4] (iD)

Abstract

Objective: Some microorganisms, i.e., *Candida albicans*, have been associated with cancer onset and development, although whether the fungus promotes cancer or whether cancer facilitates the growth of *C. albicans* is unclear. In this context, microbial-derived molecules can modulate the growth and resistance of cancer cells. This study isolated extracellular lipids (ECL) from a 36-h *Candida albicans* biofilm incubated with oral dysplastic (DOK) and neoplastic (SCC 25) cells, which were further challenged with the topoisomerase I inhibitor camptothecin (CPT), a lipophilic anti-tumoral molecule. Methodology: ECL were extracted from a 36-h *Candida albicans* biofilm with the methanol/chloroform precipitation method and identified with Nuclear Magnetic Resonance (1H-NMR). The MTT tetrazolium assay measured ECL cytotoxicity in DOK and SCC 25 cells, alamarBlue™ assessed cell metabolism, flow cytometry measured cell cycle, and confocal microscopy determined intracellular features. Results: Three major classes of ECL of *C. albicans* biofilm were found: phosphatidylinositol (PI), phosphatidylcholine (PC), and phosphatidylglycerol (PG). The ECL of *C. albicans* biofilm had no cytotoxic effect on neither cell after 24 hours, with a tendency to disturb the SCC 25 cell cycle profile (without statistical significance). The ECL-induced intracellular lipid droplet (LD) formation on both cell lines after 72 hours. In this context, ECL enhanced cell metabolism, decreased the response to CPT, and modified intracellular drug distribution. Conclusion: The ECL (PI, PC, and PG) of 36-h *Candida albicans* biofilm directly interacts with dysplastic and neoplastic oral cells, highlighting the relevance of better understanding *C. albicans* biofilm signaling in the microenvironment of tumor cells.

Keywords: *Candida albicans*. Biofilms. Lipids. Oral cancer.

Corresponding address:
Paula Aboud Barbugli
Universidade Estadual Paulista (UNESP) - Faculdade de Odontologia - Departamento de Materiais Dentários e Prótese - Araraquara 14801-903 - Brasil.
Phone: +55 16 3301-6300
e-mail: paula.barbugli@unesp.br

[1]Universidade Estadual Paulista (UNESP), Faculdade de Ciências Farmacêuticas, Departamento de Análises Clínicas, Araraquara, Brasil.
[2]Universidade Estadual Paulista (UNESP), Instituto de Química, Departamento de Bioquímica e Química Orgânica, Araraquara, Brasil.
[3]Universidade de Araraquara (UNIARA), Departamento de Saúde e Ciências Biológicas, Araraquara, Brasil.
[4]Universidade Estadual Paulista (UNESP), Faculdade de Odontologia, Departamento de Materiais Dentários e Prótese, Araraquara, Brasil.

Introduction

Many microorganisms, which are critical for oral microenvironment balance, form the oral microbiome. The microbiota residing in the oral cavity prevents the establishment of pathogenic microbes, working as a microbial antagonist.[1] Oral microbiome disruption has affected the course of oral diseases. The microbiome is affected by host immunity, therapies and drugs,[2] and latrogenic environmental changes, such as orthodontic appliances, dental restorations, implants, and dentures.[3]

The association between biofilms and cancer has been recently contemplated, particularly biofilms developed by oral plaque microorganisms, such as *Fusobacterium nucleatum*[4] and *Pseudomonas aeruginosa.*[5] The development of microbial biofilms in either cancer patients or a healthy host correlates to pro-oncogenic features such as E-cadherin loss, increased interleukin-6, and the subsequent activation of the STAT3 transcription factor.[6] These characteristics highlight the significance of understanding biofilm patterns during cancer onset, development, resistance, and prognosis.

Candida albicans is among the most common opportunistic pathogens that can colonize nearly every human tissue, causing severe invasive infections. The main virulence factor is its ability to produce biofilms. The structure of *C. albicans* biofilm includes proteins (55%), carbohydrates (25%), lipids (15%), and nucleic acids (5%).[7]

Clinically, *C. albicans* biofilms are associated with oral candidiasis and *Candida* leukoplakia.[8] The literature reports that oral yeast colonization is significantly higher in oral cancer than in non-oral cancer patients.[9] However, whether the fungus promotes cancer or whether cancer facilitates the growth of *C. albicans* is unclear; therefore, the cellular signaling between *C. albicans* and oral cancer cells remains under investigation.[10] In this context, *C. albicans* can produce carcinogenic compounds, i.e., nitrosamines, which bind to DNA and form adducts that cause genomic instability, activate oncogenes, and initiate cancer development.[6,10] Moreover, *C. albicans* up-regulates oncogenes, potentiates a pre-malignant phenotype, and participates in the early and late stages of malignant promotion and progression of oral cancer.[10,11]

The investigation of the interaction of microorganisms

and their metabolites with hosts, contributing to tumorigenesis and affecting treatment success or failure, is a currently relevant topic.[12] In a tumor microenvironment, lipid molecules (i.e., phospholipids, fatty acids, triglycerides, sphingolipids, and cholesterol) work as secondary messengers and energy storage, such as lipid droplet (LD) vesicles. LDs are essential organelles found in every cell type, from prokaryotes to eukaryotes, and proposed to be involved as hallmarks of cancer progression and resistance.[13,14]

Thus, the main goal of this investigation was to verify the presence or absence of interaction between extracellular lipids (ECL) secreted by *C. albicans* biofilms and dysplastic and neoplastic oral cells, considering the high prevalence of this fungal biofilm in the oral cavity of cancer patients and the relevance of lipids in the tumor cell microenvironment and treatment resistance.

Methodology

Strain and media

This study used the SC 5314 (ATCC™ MYA-2876™) *Candida albicans* strain. *C. albicans* cultures were maintained in Sabouraud dextrose agar (SDA; Neogen; Lansing, Michigan, USA) supplemented with chloramphenicol (1 mg/L). For storage, the tubes were maintained at -80°C in a yeast nitrogen base with 20% (v/v) glycerol (YNB; Difco; Sparks, Maryland, USA).

Biofilm growth and characterization

Candida albicans biofilms were developed in 75-cm^2 cell culture flasks and grown overnight at 37°C in YNB. Then, cell suspension was standardized to 1×10^7 CFU/mL (OD$_{540nm}$, 0.845) to form the pre-inoculum. For the inoculum, 1 mL of the pre-inoculum was diluted in 10 mL of fresh YNB medium and grown for eight hours. When the inoculum reached the logarithmic phase (OD$_{540nm}$ 0.520), it was washed twice in phosphate-buffered saline (PBS; 1.37 M NaCl, 27 mM KCl, 100 mM Na$_2$HPO$_4$, 18 mM KH$_2$PO$_4$) and centrifuged at 3,200 $\times$ *g* at 4°C. The pellet was resuspended in 20 mL of fresh RPMI-1640 medium (Sigma-Aldrich; Saint Louis, Missouri, USA) and transferred to 75-cm^2 flasks for the adhesion phase, for 90 minutes at 37°C and 55 rpm. Next, the flasks were washed twice with PBS to remove non-adherent cells. Finally, the biofilms were incubated for 36 hours in 20 mL of fresh RPMI-1640

at 37°C in an orbital shaker (55 rpm). After biofilm growth, the thickness was characterized by double-staining with SYTO9 (green fluorescent nucleic acid stain) and concanavalin-a (cell surface probe) Alexa Fluor 594-conjugated (Invitrogen; Eugene, Oregon, USA) and analyzed with confocal laser scanning microscopy (CLSM). The colonies were counted (CFU) with a serial dilution of 1:1000 of the detached biofilm in sterile PBS. The diluted solution was cultured in an SDA plate and counted after 24 hours. The extracellular components were obtained after 36 hours of biofilm growth. Then, the cultures were gently detached with a cell scraper (Corning Inc., code #3011), preventing fungal cell disruption, combined with the medium (secreted molecules), gently homogenized with a serological pipette, collected, and filtered with a 0.22-µm low protein binding filter (SFCA, Corning; Oneonta, New York, USA). This filtered solution was used for all further assays. The pH was measured with a Qualxtron bench pH meter, model QX 1500 Plus.

Lipid extractions

The extracellular lipids (ECL) in the previously described filtered solution were extracted with the methanol/chloroform precipitation method (2:1, v/v). Cooled methanol (-20°C) was added to the filtered solution. Next, chloroform was added and incubated at room temperature for one hour. After incubation, the lipid-containing phase was collected and dried overnight at room temperature to ensure solvent elimination. Finally, the pellet was suspended in 1 mL of ethanol P.A. and stored at -20°C.

Lipid ^{1}H-NMR analysis

In all experiments, the ECL pool was previously obtained from six (n=6) 36-h-biofilm cultures performed in independent biological replicates. The ECL pool of C. albicans biofilms was measured with the sulfo-phospho-vanillin method.[15] A lyophilized sample from the ECL pool was resuspended in DMSO-d6 for ^{1}H-NMR analysis. A Bruker Advanced III HD 600 spectrometer was used. The Mestre Nova software analyzed the spectrograms.

Oral squamous cells

DOK cells (Sigma-Aldrich, ECACC™ dysplastic oral keratinocyte) were cultured on 75-cm² cell culture flasks (Corning; Oneonta, New York, USA) in Dulbecco's modified Eagle's medium (DMEM; Lonza; Walkersville, Maryland, USA) supplemented with hydrocortisone (5

µg/mL; Sigma-Aldrich; Saint Louis, Missouri, USA) and fetal bovine serum (10% FBS; Gibco; Brazil). SCC 25 cells (ATCC™ primary tongue carcinoma) were cultured in a mixture of DMEM/F-12 medium (1:1) supplemented with HEPES (15 mM), hydrocortisone (400 ng/mL), sodium pyruvate (0.5 mM), and FBS (10%; Gibco; Brazil). The cells were used in the third passage in all the experiments. In a previous study by our research group, 36-h C. albicans biofilms induced the death of normal oral epithelial cells, especially the caspase-3 pathway.[16] Hence, this study did not investigate normal cell phenotypes.

Cell culturing with ECL of C. albicans biofilms

The cells were cultured as described above. DOK and SCC 25 cells were seeded in 24-well plates (Corning; Oneonta, New York, USA) with 40,000 cells/well. After 24 hours, the medium was replaced with keratinocyte basal medium (KBM-Gold; Lonza; Walkersville, Maryland, USA) supplemented with transferrin, insulin, hydrocortisone, epinephrine, gentamicin (Lonza; Walkersville, Maryland, USA), and 0.1% fatty acid-free bovine serum albumin (BSA) (Sigma-Aldrich; Saint Louis, Missouri, USA). Finally, the cells were incubated for 24 and 72 hours at 37°C with 5% CO_2. The controls were a) standard cell culture conditions and b) vehicle control (ethanol v/v) and experimental conditions (ECL v/v). The literature[7] reports a 15% maximum of lipids in C. albicans biofilms and previous findings of a non-cytotoxic 2% ethanol percentage (data not shown). Therefore, this study used a maximum amount of 2% (v/v) of ECL to stimulate DOK and SCC 25 cells.

MTT assay

Cell viability was measured with 3-(4,5-Dimethylthiazol-2-yl)-2,5-diphenyltetrazolium bromide assay (MTT assay; Sigma-Aldrich; Saint Louis, Missouri, USA), as previously described.[17] The assay was conducted after 24 hours of cell culturing with ECL of C. albicans biofilms (1% and 2% v/v). A standard control was performed with the cells under normal culture conditions. The vehicle control (1% and 2% ethanol) was also performed. The experiments occurred in four replicates on three independent occasions (n=12).

Cell cycle assay by flow cytometry

DOK and SCC 25 cells (2.5 × 10⁵ cells/well) were seeded into six-well plates (Corning™, NY, USA) in triplicate (n=3) and cultured for 24 hours with ECL of

C. albicans biofilms (2% v/v), as previously described. For the control, the cells were grown under standard conditions. The monolayer was dissociated and detached with Accutase (Sigma-Aldrich™, St. Louis, MO, USA) for 10 minutes at 37°C. Next, cells were centrifuged at 400× *g* for five minutes at 4°C. The pellet was resuspended in 100 µL of PBS and received 900 µL of chilled 70% ethanol. The cells were incubated overnight at 4°C. Then, the suspension was centrifuged at 700× *g* for five minutes at 4°C. The supernatant was discarded and the pellet was resuspended in 100 µL of a cell cycle solution (3.4 mM of tris HCl, pH 7.4; 0.1% Triton X-100; 700 U/L of RNAse (DNAse free)), 10 mM of NaCl (Sigma-Aldrich™, St. Louis, MO, USA), and 30 µg/mL of propidium iodide (Invitrogen™, Thermo Fischer Scientific Inc., MA, USA). The tubes were incubated for 20 minutes on ice and protected from light. The suspension was transferred to a cytometry tube and subjected to flow cytometry analysis (BD FACSAria™ III cell sorter). A side-scatter (SSC) versus forward-scatter (FSC) located the homogeneous cell population with the BD FACS Diva software. This population originated from an SSC-A x SSC-W dotplot, followed by an FSC-A x FSC-W graphic, to exclude debris and doublets. The PE-A × PE-W dotplot graph detected 10,000 events. The Watson Pragmatic model of FlowJo™ Software - version 10 analyzed the distribution of cell cycle phases.

Confocal laser scanning microscopy (CLSM)

Nile Red (2 mg/mL; Sigma-Aldrich; Saint Louis, Missouri, USA) staining identified lipids in *C. albicans* biofilms and lipid droplet (LD) vesicles in oral cell cultures.[18,19] *C. albicans* biofilm was grown in six-well plates (Falcon; Durham, North Carolina, USA). After 36 hours, the Nile Red solution was added and incubated at 37°C for 10 minutes. CLSM detection used a Carl Zeiss LSM 800 confocal microscope. The parameters for detecting neutral lipids were 488 nm excitation and up to 540 nm emission (yellow to green fluorescence), and for polar lipids, 561 nm excitation and above 650 nm emission (red fluorescence). All experiments occurred in triplicate on two different occasions (n=6). For oral cells, the Nile Red stock solution was diluted in acetone P.A. (2 mg/mL, use 1:1000). LD formation was evaluated only after 72 hours of oral cell culturing with ECL of *C. albicans* biofilms, according to the literature.[20] After 72 hours, the oral cells were washed with PBS. Subsequently, each well received 1 mL of fresh culture medium and 1 µL of Nile Red stock solution. Cells were incubated for 10 minutes. Then, CLSM detected LD formation in oral cells.[19]

Camptothecin challenge assay

Camptothecin (CPT) is a lipophilic molecule effective against many types of tumors. The molecular target of CPT is human DNA topoisomerase I (topo I). CPT forms a (topo)-I-CPT-DNA covalent complex, mediating DNA damage and leading cells to apoptosis.[21] Hence, CPT became an anti-tumoral lipophilic drug for challenging oral cells. DOK and SCC 25 cells were seeded at 40,000 cells/well (24-well plates) in KBM supplemented with transferrin, insulin, hydrocortisone, epinephrine, gentamicin (Lonza; Walkersville, Maryland, USA), and 0.1% (v/v) fatty acid-free BSA (Sigma-Aldrich; Saint Louis, Missouri, USA). *C. albicans* lipids (2% v/v) were added to the experimental samples for 72 hours. Then, the wells were washed with PBS and received fresh KBM without BSA. The topoisomerase I inhibitor CPT (10 µg/mL) (Sigma-Aldrich; Saint Louis, Missouri, USA) was used for the challenge assay (four hours of incubation with CPT). The controls were a) standard cell culture conditions b) vehicle control (ethanol 2% v/v), c) ECL of *C. albicans* biofilms 2% v/v, d) ECL of *C. albicans* biofilms 2% v/v + 10 µg/mL of CPT, and e) 10 µg/mL of CPT. All experiments occurred in four replicates on three independent occasions (n=12).

AlamarBlue™ assay

The alamarBlue™ assay quantified cellular metabolism. After the CPT challenge assay, 100 µL of alamarBlue™ (Invitrogen; Eugene, Oregon, USA) were added to each well and incubated for four hours at 37°C with 5% CO_2. A Fluoroskan FL (Thermo Fischer Scientific Inc., MA, USA) measured fluorescence at 545 nm excitation and 590 nm emission.

Camptothecin uptake and co-localization assay

Confocal laser scanning microscopy (CLSM) identified the intracellular co-localization of the CPT drug in LD vesicles. After the CPT challenge assay, DOK and SCC 25 cells were washed with PBS once, and each well received fresh cell culture media. Only cells treated with CPT, previously incubated with ECL of *C. albicans* or not, were evaluated in this assay. Images were obtained with a CLSM Carl Zeiss LSM 800. The CLSM parameters were brightfield and 405 nm laser range up to 470 nm for CPT uptake detection. The LD double staining co-localizing protocol used 488 nm

and 561 nm laser sources. All experiments occurred in triplicate on two different occasions (n=6).

Statistical analysis

GraphPad Prism vs 8.0 analyzed all the data in this study. All tests considered a 5% significance level. The Shapiro-Wilk normality test analyzed the data, which presented a normal distribution. The data were subjected to one-way ANOVA with Tukey's post-test to compare the groups.

Results

The 3D biofilm architecture of *Candida albicans* was shown with confocal laser scanning microscopy (CLSM) after 36 hours of development. The biofilm was stained with SYTO9 and concanavalin-a at 594 nm, reaching a thickness of around 121.88 µm (Figure 1.A). The biofilms grew to 8.11 ± 0.24 Log_{10} (corresponding to 3.72×10^8 CFU/mL), and the average pH was 6.68 ± 0.12 (SD). These results came from six independent biological replicates (n=6).

A Nile Red stain identified lipids in fresh 36-h biofilm cultures (Figure 1.B). Neutral (Figure 1.B.a) and polar (Figure 1.B.b) lipids were detected in the 36-h biofilm. Image merging allowed identifying lipid storages in the biofilm (Figure 1.B.c) and detailing them (Figure 1.B.d). Then, the extracellular lipid (ECL) pool produced by the 36-h *C. albicans* biofilm was quantified, reaching a concentration of 3.5 mg/mL. All further assays were performed with this ECL pool.

The ^{1}H-NMR spectroscopy analyzed the ECL pool to identify its main composition. Figure 2 shows the peaks corresponding to the hydrogen resonance of lipids. The hydrogen from the CH_3-free aliphatic terminal, common to all lipids, corresponds to the weak peak at 0.8 ppm (Figure 2, a). The hydrogen from methylene protons of aliphatic chains (-CH_2) n, β-methylene protons of carbonyl $-OCO-CH_2-CH_2-$, and methylene protons in the α-position of $-CH_2-CH=CH-$ double bond peaks appear at 1.2-2.50 ppm (Figure 2, b). The CH_2CO residues peak at 2.53 ppm (Figure 2, c). The methylene protons of the heteroatom connected to phosphorus (CH_2-O-P), typical of phospholipids, appear at 4.43 ppm (Figure 2, d), as well $-C1H_2$ in the glycerol backbone in phospholipids (Figure 2, c).[22] The methyl protons of charged nitrogen $N-(CH_3)^{+3}$, typical of choline, appear at 3.36 ppm (Figure 2,

e).[22,23] The C_6HOH of inositol and CH_2O of glycerol, typical of glycolipids, appear at 3.42 ppm (Figure 2, f). Double bond protons with cis conformation in the aliphatic chain ($-CH=HC$) appear at 5.47 ppm (Figure 2, g).[23] The ^{1}H-NMR strongly suggested that phosphatidylinositol (PI), phosphatidylcholine (PC), and phosphatidylglycerol (PG) lipids prevailed in the extracts.

The ECL pool helped explain the presence or absence of direct interaction between pre-malignant (DOK cells) and malignant (SCC 25) oral cells ECL of *C. albicans* biofilms. A cytotoxicity curve was made for both cells using the vehicle control (ethanol), achieving the optimal amount (2% v/v) of solvent (ethanol) for the next steps (data not shown). DOK and SCC 25 cells were incubated for 24 hours with ECL of *C. albicans* biofilms (1% and 2% v/v). A statistical difference (**$p<0.01$) in the cell viability (MTT assay, n=12) of DOK cells when exposed to ECL 2% (v/v) was found, but not to ECL 1% (v/v) (Figure 3. A). Even when verifying differences in the cell viability assay, the cell cycle profile (n=3) of DOK cells did not change (Figure 3.a blue arrows). The SCC 25 cells showed a difference between ECL (1% and 2% v/v) and the control in the MTT cell viability assay (n=12), *$p<0.05$ (Figure 3. B). At a higher ECL concentration (2% v/v), SCC 25 cells showed a different cell cycle profile, with a G1 phase enlargement and a G2/M phase flattening, without statistical significance (n=3) (Figure 3.b, red arrows compared to blue arrows).

As for intracellular changes, a CLSM Nile Red assay was performed for 72 hours after the incubation of DOK and SCC 25 cells with ECL 2% (v/v) of *C. albicans* biofilms (n=6). First, control cells (Figure 4 column A) and vehicle control cells (Figure 4 column B) did not show significant changes in the amount and size of intracellular lipid droplets (LD). The ECL group induced an extensive intracellular LD formation in DOK and SCC 25 cells compared to controls (Figure 4 column C, showing bright yellow spots – white arrows).

DOK and SCC 25 cells were challenged with the lipophilic topoisomerase I inhibitor camptothecin (CPT), attempting to understand whether the ECL of *C. albicans* biofilms could change cellular susceptibility to anti-tumoral drugs. DOK cells showed a difference between the control and ECL 2% (****$p<0.0001$) and the control and CPT (***$p<0.001$). There was a difference between ECL 2% and CPT (****$p<0.0001$) and ECL 2% and ECL 2% + CPT (***$p<0.001$),

demonstrating mitigation of the CPT effect. SCC 25 cells showed a difference between the control and ECL 2% (***$p<0.001$) and ECL 2% + CPT (****$p<0.0001$) and CPT (*$p<0.05$). Both treated ECL 2% cells (ECL 2% and ECL 2% + CPT) showed a difference compared to CPT (for both groups, ****$p<0.0001$). However,

no differences between ECL 2% and ECL 2% + CPT were found, demonstrating resistance to CPT when previously culturing cells with ECL 2%.

CPT uptake was studied with CLSM (n=6). Figures 5.a (DOK cells) and 5.b (SCC 25 cells) showed that the ECL of *C. albicans* biofilms did not change the amount
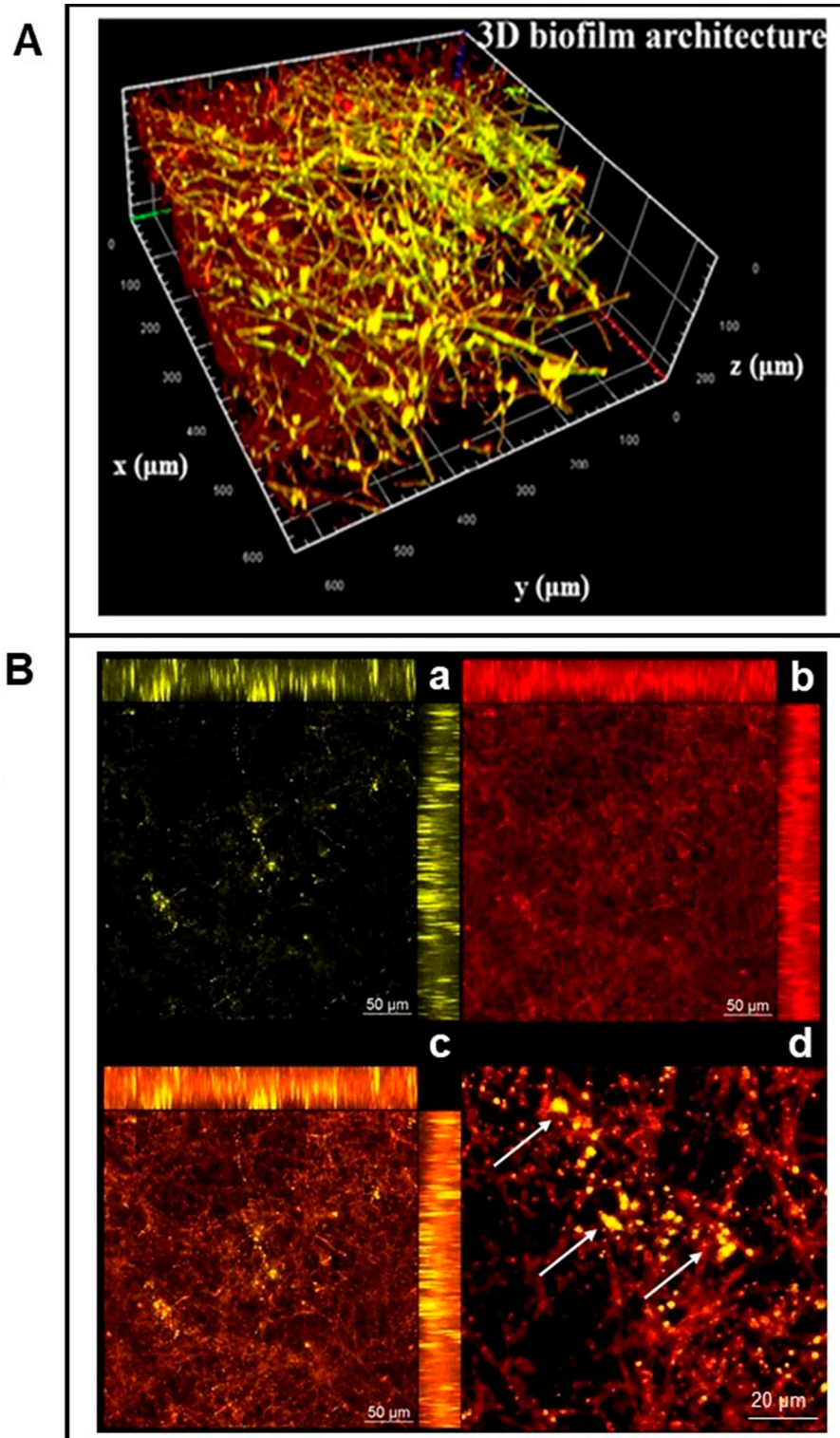
Figure 1- *Candida albicans* biofilm characterization. (Upper panel) A. CLSM of a 3D architecture of the 36-h *C. albicans* biofilm stained with SYTO9 and concanavalin Alexa-Fluor 594 nm. The biofilm presented a green-yellow-red fluorescence and thickness of 121.88 µm. (Down panel) B. CLSM images of the 36-h *C. albicans* biofilm with Nile Red staining. (B.a) Neutral lipids stained in yellow. (B.b) Polar lipids stained in red. (B.c) Lipid storage (Gold-yellow intracellular spots – white arrow). (B.d). Detailed lipid storage. (n=6).
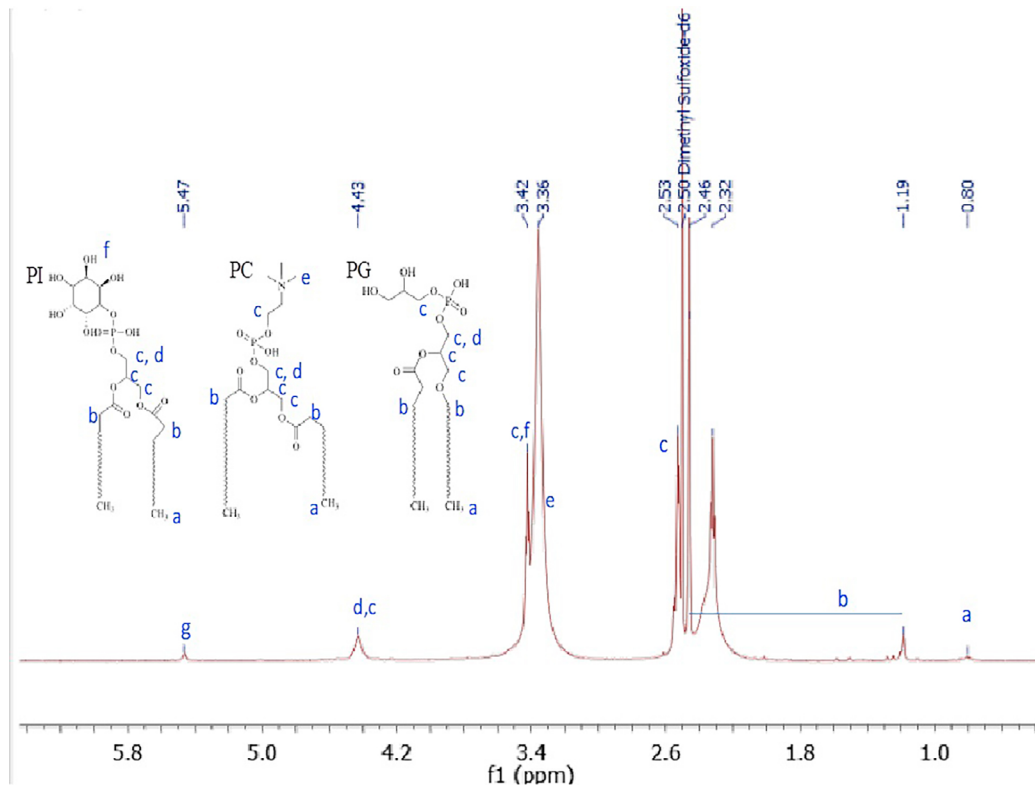
Figure 2- Spectrogram of lipids (ECL) extracted from *C. albicans* biofilm. Resonance was performed from a lyophilized sample of *C. albicans* lipids previously extracted from six biofilms (n=6). The sample was resuspended in DMSO for ¹H-NMR analysis. (a) CH₃ residues. (b) CH₂ residues from methylene protons of aliphatic chains –(CH₂) n, β-methylene protons of carbonyl –OCO−CH₂−CH₂−, and methylene protons in the α-position of –CH₂−CH=CH− double bonds. (c) CH₂CO residues. (d) Methyl protons of charged nitrogen N-(CH₃)⁺³, C-OH (C1, C4) of phosphatidylinositol, and glycerol and CH₃ of methyl glycerol. The identified lipids were phosphatidylinositol (PI); phosphatidylcholine (PC), and phosphatidylglycerol (PG).
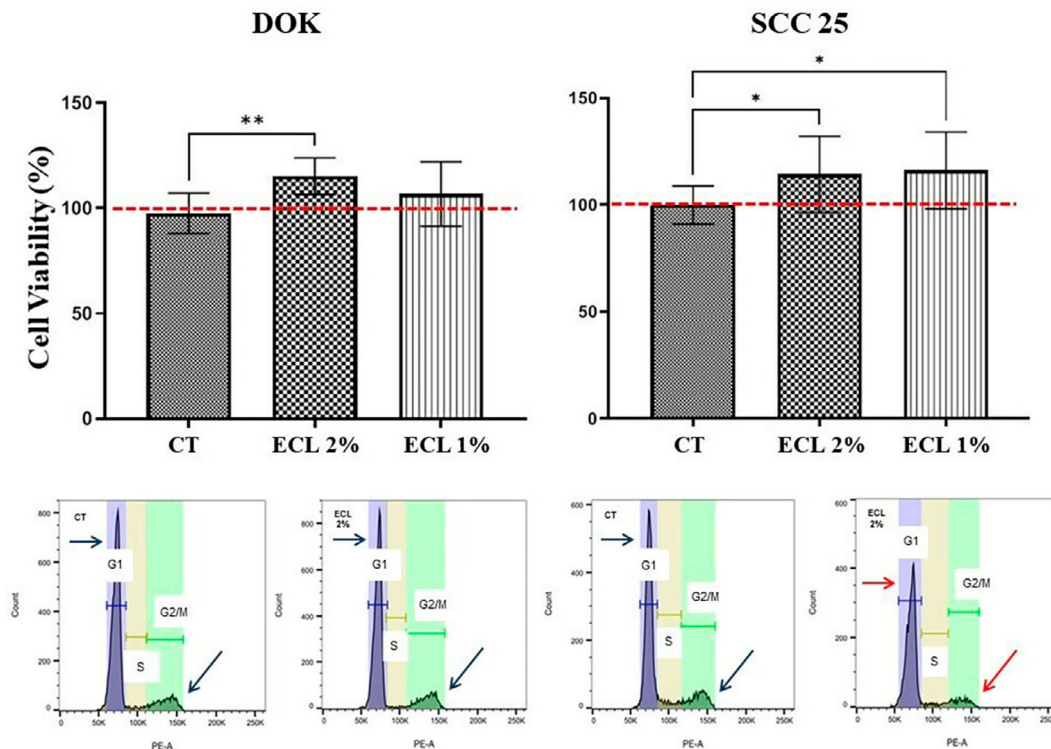
Figure 3- Cell viability and cell cycle profile. The MTT assay assessed cell viability (n=12). (A) Cell viability assay for DOK cells. A statistical difference between the group exposed to ECL 2% (v/v) and the control (**p<0.01) was found. (B) Cell viability assay for SCC 25 cells. A statistical difference between both groups exposed to ECL and the control (*p<0.05) was found. The cell cycle assay of DOK cells (n=3) (a) showed no tendency to change the cell cycle profile between CT and ECL (blue arrows). SCC 25 cells (n=3) (b) showed a tendency to disturb the cell cycle profile, with a G1 phase enlargement and a G2/M phase flattening, without statistical significance (n=3), comparing the CT (blue arrow) and ECL (red arrow) groups.
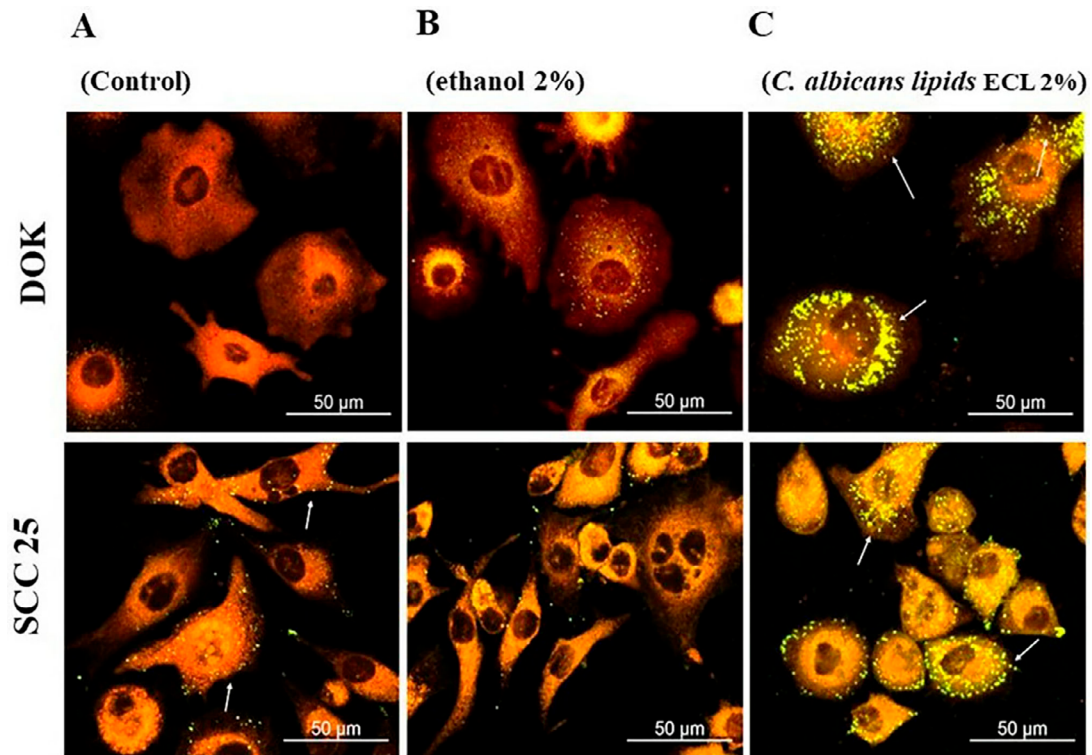
Figure 4- Confocal laser screening microscopy (CLSM) for DOK and SCC 25 cells cultured with ECL of *C. albicans* biofilm. CLSM of LD in DOK and SCC 25 cells after culturing for 72 hours with ECL (2% v/v) of *C. albicans*. (A) DOK and SCC 25 cells (control), (B) DOK and SCC 25 cells (vehicle), and (C) DOK and SCC 25 cells (ECL 2% v/v), LD vesicles (arrows), n=6.
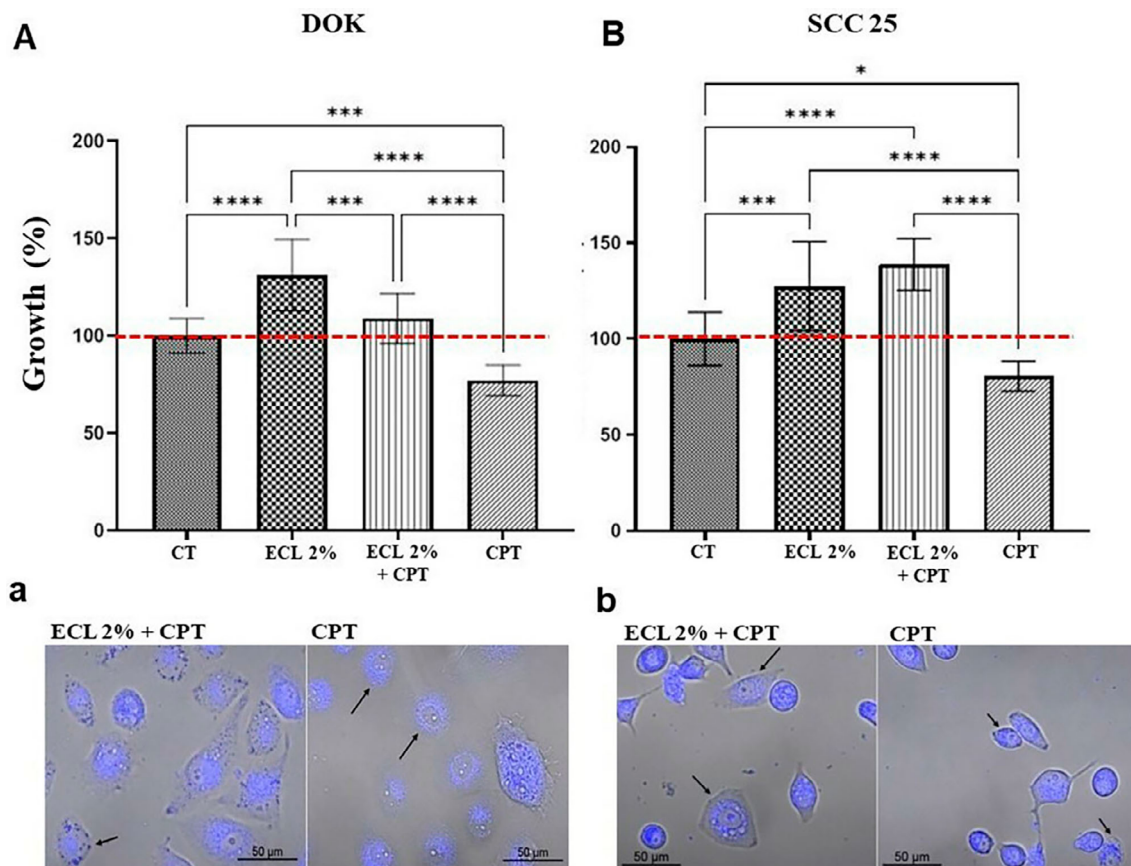
Figure 5- AlamarBlue and CPT uptake of DOK and SCC 25 cells cultured with ECL of *C. albicans* biofilm. DOK and SCC 25 cells were cultured with ECL of *C. albicans* for 72 hours. Then, the cells were challenged with the topoisomerase I inhibitor CPT for another four hours, followed by the alamarBlueTM assay (n=12). DOK cells (A) showed statistical differences between all groups. SCC 25 cells (B) showed statistical differences between all groups, except for the cells exposed to ECL 2% v/v and ECL 2% v/v + CPT (*p<0.05; ***p<0.001; ****p<0.0001). CPT uptake with brightfield and 405 nm fluorescence emission (arrows) for (a) DOK (n = 6) and (b) SCC 25 (n=6) cells.
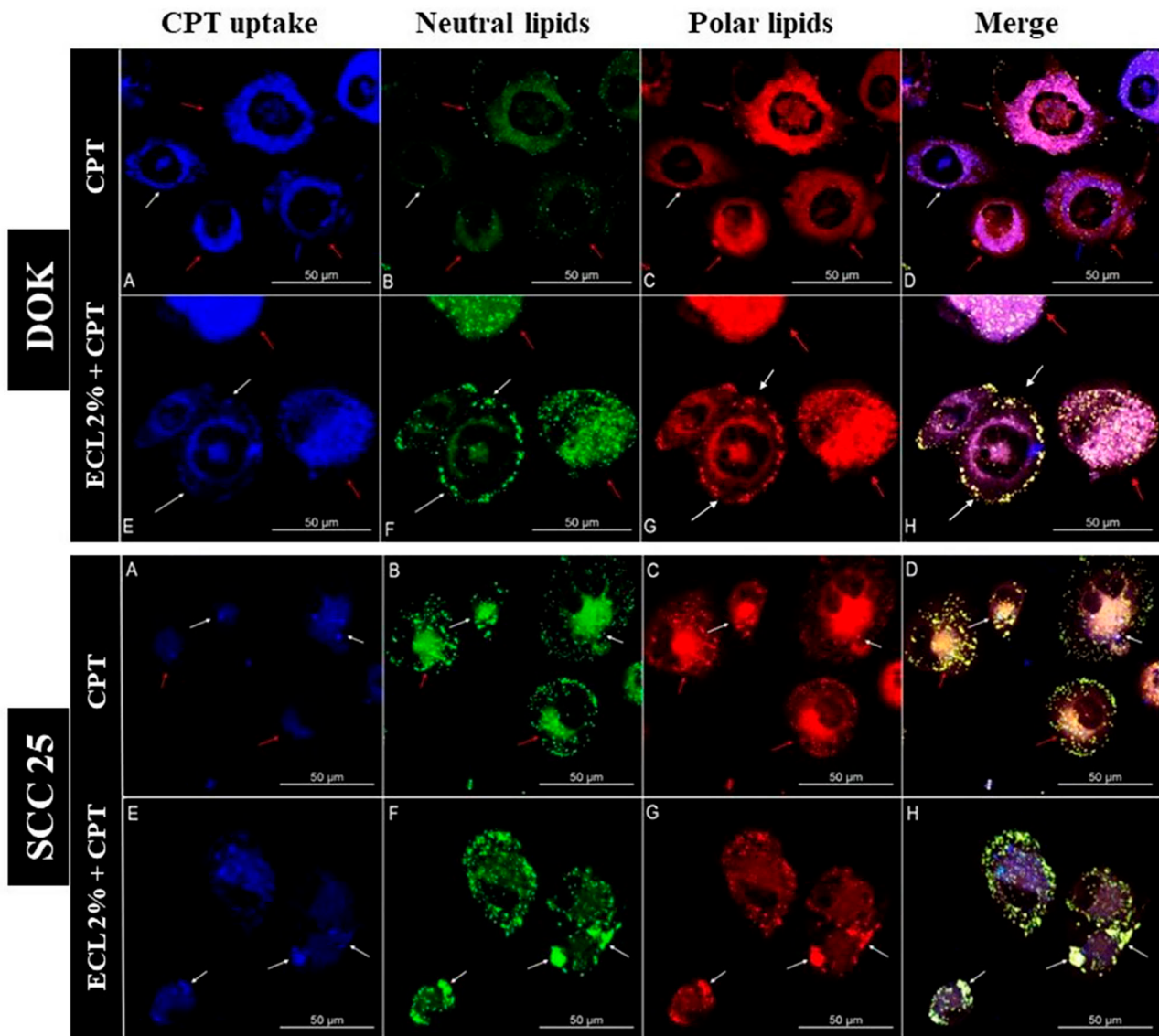
Figure 6- Cell double staining of CPT and 2% ECL of 36-h *C. albicans* biofilms with Nile Red and high-resolution CLSM. DOK cells (upper panel). CPT detection (A - blue panel white arrows). Nile Red neutral lipids (B - green panel). Nile Red polar lipids (C - red panel). Co-localization of CPT and LD (D – merged panel, white arrows) (n=6). SCC 25 cells (down panel). CPT detection (A – blue panel, white arrows). Nile Red neutral lipids (B - green panel). Nile Red polar lipids (C - red panel). Co-localization of CPT and LD (D - merged panel, white arrows) (n=6). Red arrows show no co-localization between CPT and LD. White arrows show a positive co-localization between CPT and LD.

of CPT internalization. However, a high-resolution CLSM tool with a Nile Red double staining (n=6) detected a different pattern of CPT intracellular distribution (Figure 6). In the absence of ECL incubation, DOK cells had a higher perinuclear CPT retention (Figure 6. upper panel A - red arrows) than the cytoplasmic distribution of the ECL group (Figure 6. upper panel E - white arrows). A positive co-localization with the formed LD and the CPT (Figure 6. upper panels F, G, and H – yellow to white spots, respectively) was found, with a positive accumulation of CPT in LD. This behavior was poorly detected without ECL (Figure 6. upper panels C, D, and E). For SCC 25 cells, cytoplasmic aggregates were more pronounced in the group previously cultured with ECL of *C. albicans* biofilms (Figure 6. down panel

A compared to E – white arrows). These aggregates showed a positive CPT-LD co-localization (Figure 6. down panels B, C, D, F, G, H – white arrows) with a large amount and size of yellow to white spots in the group previously cultured with ECL of *C. albicans* (Figure 6. down panels F, G, H – white arrows). Red arrows show no co-localization between CPT and LD. White arrows show a positive co-localization between CPT and LD.

Discussion

The opportunistic fungus *C. albicans* has received

much attention over the last decade, mainly due to its ability to produce biofilms. Some fingerprints, i.e., lipid molecules, from the extracellular matrix of *C. albicans* biofilms play a critical role in infection and fungal resistance.[7] Most of these molecules consist of neutral classes of free fatty acids, triacylglycerols, glycerolipids, sphingolipids, and phospholipids (i.e., phosphatidylethanolamine, phosphatidylserine, and phosphatidylinositol). The SC 5314 strain showed significant differences in the distribution of lipid classes between biofilm and planktonic growth, i.e., biofilms with higher lipid levels than planktonic cells.[24]

It is worth noting that *C. albicans* infects hosts not as free-living planktonic organisms, but as a multicellular biofilm, developing chronic infections mainly in the oral cavity. Chronic inflammation has been linked to many carcinogenesis stages,[25,26] and biofilm formation has been attributed to a potential etiological role in the development of some cancers.[27-29] Recent clinical studies have linked fungi (e.g., *C. albicans*) and cancer, claiming the need for more *in vitro* and *in vivo* studies in this area.[30,31]

In a tumor microenvironment, the resident microbiota and its metabolites trigger metabolic signaling pathways, which further promote or suppress the malignant behavior of host cells.[32] In this study, the entire fresh 36-h *C. albicans* biofilm produced lipid molecules, as Radulovic, et al described.[33] (2013). Phosphatidylcholine (PC), phosphatidylglycerol (PG), and phosphatidylinositol (PI) molecules were the three major identified lipid classes, named extracellular lipids (ECL), and these findings correlate to previous studies.[24,34]

The ECL in this study induced lipid droplet (LD) formation in DOK and SCC 25 cells. LD vesicles represent energy storage readily available to support anoikic resistance and cancer cell invasiveness.[20] LD is involved in lipid and protein storage, transportation, and degradation, contributing to many diseases, including cancer. Regarding *C. albicans* infections, unknown mechanisms described LD biogenesis in macrophages and hepatocytes in a rat model,[35] and we found no descriptions for oral dysplastic or neoplastic cells.

Therefore, the significance of LD has provided a compelling insight into cancer treatment. LD is present in some breast and colon adenocarcinomas resistant to chemotherapeutical drugs.[14,36] Many mechanisms related to the environment explain the resistance

mediated by lipids in cancer cells. For example, resistance to tyrosine kinase inhibitors is associated with new lipid biosynthesis.[37] Drug-resistant cancer cells have shown increased LD numbers. These organelles were postulated to sequester hydrophobic agents, reducing drug effectiveness and activating the ERK/Akt/mTOR survival pathway.[37,38] In the presence of ECL of *C. albicans* biofilm, the anti-tumoral effect of the camptothecin (CPT) lipophilic drug was mitigated and abolished in DOK and SCC 25 cells, respectively. This cellular behavior occurred with different patterns of intracellular drug uptake, mainly inside the LD vesicles induced by *C. albicans* lipids. Also, LD was already described as a positive marker of malignant phenotype progression.[39] Thus, a positive correlation between lipids (PC, PG, and PI) of *C. albicans* biofilms and the *in vitro* LD formation in oral dysplastic and neoplastic cells addresses the relevance of better understanding this pathogen-host interaction in a tumor environment.

Overall, our findings and those from recent clinical studies[30,31] require further investigation. We should note that the tumoral microenvironment is a complex network that includes many tissues, immune cells, and the microbiome formed by many bacteria, fungi, and viruses living in the same environment, thus contributing to cancer.

Conclusion

This study described for the first time the direct interaction between lipids of *Candida albicans* biofilms and oral dysplastic and neoplastic cells. Phosphatidylcholine, phosphatidylglycerol, and phosphatidylinositol were identified and enhanced cellular metabolism, lipid droplet formation, and anti-tumoral drug resistance. Thus, this study addressed the relevance of better understanding the signaling of *C. albicans* biofilms in the oral tumor microenvironment.

Authors' contributions

Marin-Dett, Freddy Humberto: Conceptualization (Equal); Data curation (Equal); Formal analysis (Equal); Investigation (Equal); Methodology (Equal); Validation (Equal); Writing – original draft (Lead); Writing – review & editing (Equal). **Campanella, Jonatas Erick Maimoni:** Data curation (Supporting); Formal analysis (Equal); Methodology (Supporting); Writing – original draft (Supporting). **Trovatti, Eliane:** Formal analysis (Equal); Methodology (Equal); Validation (Equal); Writing – original draft (Supporting). **Bertolini, Maria Célia:** Data curation (Equal); Formal analysis (Equal); Funding acquisition (Equal); Investigation (Equal); Supervision (Supporting); Writing – original draft (Equal). **Vergani, Carlos Eduardo:** Funding acquisition (Lead); Project administration (Equal); Supervision (Equal); Writing – original draft (Equal); Writing – review & editing (Equal). **Barbugli, Paula:** Conceptualization (Lead); Data curation (Lead); Formal analysis (Equal); Funding acquisition (Equal); Investigation (Equal); Methodology (Supporting); Project administration (Lead); Resources (Equal); Supervision (Lead); Validation (Supporting); Visualization (Supporting); Writing – original draft (Equal); Writing – review & editing (Lead).

Conflict of interest

The authors declare no conflict of interest.

Data availability statement

The datasets generated during the current study are available from the corresponding author on reasonable request.

References

1- Irfan M, Delgado RZ, Frias-Lopez J. The Oral microbiome and cancer. Front Immunol. 2020;11:591088. doi: 10.3389/fimmu.2020.591088

2- Börnigen D, Ren B, Pickard R, Li J, Ozer E, Hartmann EM, et al. Alterations in oral bacterial communities are associated with risk factors for oral and oropharyngeal cancer. Sci Rep. 2017;7(1):17686. doi: 10.1038/s41598-017-17795-z

3- Pokrowiecki R, Mielczarek A, Zaręba T, Tyski S. Oral microbiome and peri-implant diseases: where are we now? Ther Clin Risk Manag. 2017;13:1529-42. doi: 10.2147/TCRM.S139795

4- Brennan CA, Garrett WS. *Fusobacterium nucleatum:* symbiont, opportunist and oncobacterium. Nat Rev Microbiol. 2019;17(3):156-66. doi: 10.1038/s41579-018-0129-6

5- Al-hebshi NN, Nasher AT, Maryoud MY, Homeida HE, Chen T, Idris AM, et al. Inflammatory bacteriome featuring *Fusobacterium nucleatum* and *Pseudomonas aeruginosa* identified in association with oral squamous cell carcinoma. Sci Rep. 2017;7(1):1834. doi: 10.1038/s41598-017-02079-3

6- Johnson CH, Dejea CM, Edler D, Hoang LT, Santidrian AF, Felding BH, et al. Metabolism links bacterial biofilms and colon carcinogenesis. Cell Metab. 2015;21(6):891-7. doi: 10.1016/j.cmet.2015.04.011

7- Zarnowski R, Westler WM, Lacmbouh GA, Marita JM, Bothe JR, Bernhardt J, et al. Novel entries in a fungal biofilm matrix encyclopedia. mBio. 2014;5(4):e01333-14. doi: 10.1128/mBio.01333-14

8- Sokol H, Leducq V, Aschard H, Pham H-P, Jegou S, Landman C, et al. Fungal microbiota dysbiosis in IBD. Gut. 2017;66(6):1039-48. doi: 10.1136/gutjnl-2015-310746

9- Alnuaimi AD, Wiesenfeld D, O'Brien-Simpson NM, Reynolds EC, McCullough MJ. Oral *Candida* colonization in oral cancer patients and its relationship with traditional risk factors of oral cancer: a matched case-control study. Oral Oncol. 2015;51(2):139-45. doi: 10.1016/j.oraloncology.2014.11.008

10- Vadovics M, Ho J, Igaz N, Alföldi R, Rakk D, Veres E, et al. *Candida albicans* enhances the progression of oral squamous cell carcinoma *in vitro* and *in vivo*. mBio. 2022;13(1):e03144-21. doi: 10.1128/mBio.03144-21

11- Amaya Arbeláez MI, Silva AC, Navegante G, Valente V, Barbugli PA, Vergani CE. Proto-oncogenes and cell cycle gene expression in normal and neoplastic oral epithelial cells stimulated with soluble factors from single and dual biofilms of *Candida albicans* and *Staphylococcus aureus*. Front Cell Infect Microbiol. 2021;11:627043. doi: 10.3389/fcimb.2021.627043

12- Bullman S, Pedamallu CS, Sicinska E, Clancy TE, Zhang X, Cai D, et al. Analysis of *Fusobacterium* persistence and antibiotic response in colorectal cancer. Science. 2017;358(6369):1443-8. doi: 10.1126/science.aal5240

13- Buechler C, Aslanidis C. Role of lipids in pathophysiology, diagnosis and therapy of hepatocellular carcinoma. Biochim Biophys Acta Mol Cell Biol Lipids. 2020;1865(5):158658. doi: 10.1016/j.bbalip.2020.158658

14- Montopoli M, Bellanda M, Lonardoni F, Ragazzi E, Dorigo P, Froldi G, et al. "Metabolic Reprogramming" in ovarian cancer cells resistant to cisplatin. Curr Cancer Drug Targets. 2011;11(2):226-35. doi: 10.2174/156800911794328501

15- Nunes TS, Rosa LM, Vega-Chacón Y, Mima EG. Fungistatic action of N-Acetylcysteine on *Candida albicans* biofilms and its interaction with antifungal agents. Microorganisms. 2020;8(7):980. doi: 10.3390/microorganisms8070980

16- Dias KC, Barbugli PA, Vergani CE. Influence of different buffers (HEPES/MOPS) on keratinocyte cell viability and microbial growth. J Microbiol Methods. 2016;125:40-2. doi: 10.1016/j.mimet.2016.03.018

17- Dias KC, Sousa DL, Barbugli PA, Cerri PS, Salih VM, Vergani CE. Development and characterization of a 3D oral mucosa model as a tool for host-pathogen interactions. J Microbiol Methods. 2018;152:52-60. doi: 10.1016/j.mimet.2018.07.004

18- Larsen P, Olesen BH, Nielsen PH, Nielsen JL. Quantification of lipids and protein in thin biofilms by fluorescence staining. Biofouling. 2008;24(4):241-50. doi: 10.1080/08927010802040255

19- Antunes P, Cruz A, Barbosa J, Bonifácio VD, Pinto SN. Lipid droplets in cancer: from composition and role to imaging and therapeutics. Molecules. 2022;27(3):991. doi: 10.3390/molecules27030991

20- Corbet C, Bastien E, Jesus JP, Dierge E, Martherus R, Vander Linden C, et al. TGFβ2-induced formation of lipid droplets supports acidosis-driven EMT and the metastatic spreading of cancer cells. Nat Commun. 2020;11(1):454. doi: 10.1038/s41467-019-14262-3

21- Liu LF, Desai SD, Li TK, Mao Y, Sun M, Sim SP. Mechanism of action of camptothecin. Ann N Y Acad Sci. 2000;922:1-10. doi: 10.1111/j.1749-6632.2000.tb07020.x

22- Mika A, Kaczynski Z, Stepnowski P, Kaczor M, Proczko-Stepaniak M, Kaska L, et al. Potential application of 1H NMR for routine serum lipidome analysis: evaluation of effects of bariatric surgery. Sci Rep. 2017;7(1):15530. doi: 10.1038/s41598-017-15346-0

23- Mor NC, Correia BS, Valc AL, Tasic L. A protocol for fish lipid analysis using Nuclear Magnetic Resonance Spectroscopy. J Braz Chem Soc. 2020;31(4):662-72. doi: 10.21577/0103-5053.20190230

24- Lattif AA, Mukherjee PK, Chandra J, Roth MR, Welti R, Rouabhia M, et al. Lipidomics of *Candida albicans* biofilms reveals phase-dependent production of phospholipid molecular classes and role for lipid rafts in biofilm formation. Microbiology (Reading). 2011;157(Pt 11):3232-42. doi: 10.1099/mic.0.051086-0

25- Armstrong MJ, Mullins CD, Gronseth GS, Gagliardi AR. Impact of patient involvement on clinical practice guideline development: a parallel group study. Implement Sci. 2018;13(1):55. doi: 10.1186/s13012-018-0745-6

26- Plummer M, de Martel C, Vignat J, Ferlay J, Bray F, Franceschi S. Global burden of cancers attributable to infections in 2012: a synthetic analysis. Lancet Glob Health. 2016;4(9):e609-16. doi: 10.1016/S2214-109X(16)30143-7

27- Dejea CM, Fathi P, Craig JM, Boleij A, Taddese R, Geis AL, et al. Patients with familial adenomatous polyposis harbor colonic biofilms containing tumorigenic bacteria. Science. 2018;359(6375):592-7. doi: 10.1126/science.aah3648

28- Dejea CM, Wick EC, Hechenbleikner EM, White JR, Welch JLM, Rossetti BJ, et al. Microbiota organization is a distinct feature of proximal colorectal cancers. Proc Natl Acad Sci U S A. 2014;111(51):18321-6. doi: 10.1073/pnas.1406199111

29- Deng Y, Liu SY, Chua SL, Khoo BL. The effects of biofilms on tumor progression in a 3D cancer-biofilm microfluidic model. Biosens Bioelectron. 2021;180:113113. doi: 10.1016/j.bios.2021.113113

30- Narunsky-Haziza L, Sepich-Poore GD, Livyatan I, Asraf O, Martino C, Nejman D, et al. Pan-cancer analyses reveal cancer-type-specific fungal ecologies and bacteriome interactions. Cell. 2022;185(20):3789-806.e17. doi: 10.1016/j.cell.2022.09.005

31- Dohlman AB, Klug J, Mesko M, Gao IH, Lipkin SM, Shen X, et al. A pan-cancer mycobiome analysis reveals fungal involvement in gastrointestinal and lung tumors. Cell. 2022;185(20):3807-22.e12. doi: 10.1016/j.cell.2022.09.015

32- Liu NN, Ma Q, Ge Y, Yi CX, Wei LQ, Tan JC, et al. Microbiome dysbiosis in lung cancer: from composition to therapy. NPJ Precis Oncol. 2020;4(1):33. doi: 10.1038/s41698-020-00138-z

33- Radulovic M, Knittelfelder O, Cristobal-Sarramian A, Kolb D, Wolinski H, Kohlwein SD. The emergence of lipid droplets in yeast: current status and experimental approaches. Curr Genet. 2013;59(4):231-42. doi: 10.1007/s00294-013-0407-9

34- Zarnowski R, Sanchez H, Covelli AS, Dominguez E, Jaromin A, Bernhardt J, et al. *Candida albicans* biofilm-induced vesicles confer drug resistance through matrix biogenesis. PLoS Biol. 2018;16(10):e2006872. doi: 10.1371/journal.pbio.2006872

35- Paraje MG, Correa SG, Renna MS, Theumer M, Sotomayor CE. *Candida albicans*-secreted lipase induces injury and steatosis in immune and parenchymal cells. Can J Microbiol. 2008;54(8):647-59. doi: 10.1139/w08-048

36- Santini MT, Romano R, Rainaldi G, Filippini P, Bravo E, Porcu L, et al. The relationship between 1H-NMR mobile lipid intensity and cholesterol in two human tumor multidrug resistant cell lines (MCF-7 and LoVo). Biochim Biophys Acta. 2001;1531(1-2):111-31. doi: 10.1016/s1388-1981(01)00093-2

37- Butler LM, Perone Y, Dehairs J, Lupien LE, de Laat V, Talebi A, et al. Lipids and cancer: emerging roles in pathogenesis, diagnosis and therapeutic intervention. Adv Drug Deliv Rev. 2020;159:245-93. doi: 10.1016/j.addr.2020.07.013

38- Verbrugge SE, Al M, Assaraf YG, Kammerer S, Chandrupatla DM, Honeywell R, et al. Multifactorial resistance to aminopeptidase inhibitor prodrug CHR2863 in myeloid leukemia cells: down-regulation of carboxylesterase 1, drug sequestration in lipid droplets and pro-survival activation ERK/Akt/mTOR. Oncotarget. 2016;7(5):5240-57. doi: 10.18632/oncotarget.6169

39- Cruz AL, Barreto EA, Fazolini NP, Viola JP, Bozza PT. Lipid droplets: platforms with multiple functions in cancer hallmarks. Cell Death Dis. 2020;11(2):105. doi: 10.1038/s41419-020-2297-3